Exploration of genes related to the development of cancer of unknown primary

YOSHIHIKO FUJITA[1], MARCO A. DE VELASCO[1], HIDETOSHI HAYASHI[2], KAZUHIKO NAKAGAWA[2] and KAZUTO NISHIO[1]

[1]Department of Genome Biology, Kindai University Faculty of Medicine, Osaka-Sayama, Osaka 589-8511, Japan; [2]Department of Medical Oncology, Kindai University Faculty of Medicine, Osaka-Sayama, Osaka 589-8511, Japan

Received November 19, 2024; Accepted February 21, 2025

DOI: 10.3892/or.2025.8905

Abstract. The biological basis of the development of cancer of unknown primary (CUP) remains largely unknown, with no evidence of whether a common biological basis exists at present. Our previous multicenter clinical study predicted the primary site of CUP for site-specific therapy. Concomitantly with the study, a microarray analysis of tumor mRNA samples obtained from 60 participants of the study with CUP was performed, and a gene expression profile specific to CUP was constructed. Several of the genes identified as being upregulated/downregulated in CUP could potentially be clinically useful common biomarkers of CUP. In the present study, to identify genes that may be more closely related to the development of CUP (characterized by its metastatic potential) among the upregulated genes, cell-based small interfering RNA screening was performed *in vitro*, and two genes, protein kinase DNA-activated catalytic subunit (PRKDC) and proteasome subunit β type-4 (PSMB4), were identified to be possibly involved in the metastatic ability of CUP, since knockdown of these genes resulted in reduced migration of A549 cells. These genes were further knocked down in A549 cells using short hairpin RNAs (shRNAs) and the cells were implanted into the footpad of mice. Marked suppression of the metastatic ability of implanted cells from the footpad to the popliteal lymph node (LN) was observed in cells transfected with the shRNAs for PRKDC and PSMB4. In addition, bortezomib, a proteasome inhibitor, markedly reduced the ability of cells implanted into the footpad to metastasize to the LNs, as well as cell growth at the metastatic site, compared with vehicle or NU7447 (inhibitor of PRKDC). These findings indicated that proteasomal function activation augmented the metastatic ability of malignant CUP cells.

Correspondence to: Dr Yoshihiko Fujita, Department of Genome Biology, Kindai University Faculty of Medicine, 377-2 Ohno-Higashi, Osaka-Sayama, Osaka 589-8511, Japan
E-mail: fujita@med.kindai.ac.jp

Abbreviations: CUP, cancer of unknown primary; PRKDC, protein kinase DNA-activated catalytic subunit; PSMB4, proteasome subunit β type-4

Key words: CUP, migration, lymph node metastasis, PRKDC, PSMB4, small interfering RNA, short hairpin RNA, bortezomib, proteasome

Introduction

Cancer of unknown primary (CUP) is defined as histologically confirmed metastatic cancer in which the primary site cannot be found even after extensive standard investigations (1). At present, the favorable risk subgroup for CUP includes patients with neuroendocrine carcinomas of unknown primary, peritoneal adenocarcinomatosis of a serous papillary subtype, isolated axillary nodal metastases in female patients, squamous cell carcinoma involving non-supraclavicular cervical lymph nodes (LNs), single metastatic deposit from unknown primary, and men with blastic bone metastases and prostate-specific antigen expression (2). Novel favorable subsets of CUP have emerged, including colorectal, lung and renal CUP, which underlines the importance of cancer-specific treatments (2). Patients with CUP who are categorized into the unfavorable subset (~80% of patients) receive empiric chemotherapy with a platinum-taxane regimen. However, the prognosis remains poor, with a median survival period of 6-12 months (3,4). The poor prognosis of CUP is attributable to its clinical heterogeneity originating from various types of cancers, which makes a single empiric regimen inefficient (5).

Our previous randomized controlled study (6) assessed whether site-specific therapy based on prediction of the primary site may improve the outcomes in untreated patients with CUP. Genome-wide gene expression profiling of CUP was performed in the study using a microarray to predict the primary site in each patient with CUP (6). However, substantial shortcomings have been identified in the existing research comparing site-specific treatment and empiric chemotherapy. These deficiencies include patient accrual problems (oversampling treatment-resistant tumor types and long recruitment), study design limitations (observational and problematic trials), heterogeneity among the CUP classifiers (epigenetic vs. transcriptomic profiling) and incomparable therapies (7). Treatment based on the prediction of the primary site did not lead to any improvement of the overall survival compared with

empiric chemotherapy in our previous study (6); however, gene profiling analyses of patients with CUP and comparison of the gene expression patterns in these patients with those in tumors from 24 known primary sites revealed several genes that were uniquely upregulated in CUP (8). Of the ~22,000 genes mounted on the microarray, 44 genes that were upregulated in CUPs were identified in our previous study (8).

The early metastasis in the natural history of CUP remains poorly understood. The present study identified genes that could serve a role in the metastasis in CUP. Small interfering RNA (siRNA) knockdown screens were used to assess the genes upregulated in the present CUP cohort to determine their impact on the migration of cancer cells and further characterize candidate genes using an *in vivo* metastasis model.

Materials and methods

Cell culture and reagents. The A549 human lung cancer cell line (cat. no. CCL-185) and the MDA231 breast cancer cell line (cat. no. HTB-26) were procured from American Type Culture Collection, and cultured in DMEM (Thermo Fisher Scientific, Inc.) with 10% FBS (MilliporeSigma) in accordance with the instructions provided by the suppliers. The cells were maintained in a 5% CO_2 humidified atmosphere at 37˚C.

Cell viability assay. The proliferation rate of cultured cells was analyzed using MTT (MilliporeSigma) as previously described (9). The assay was performed in triplicate where applicable.

Reverse transcription-quantitative PCR (RT-qPCR). Total RNA (1 μg) from cells, extracted using ISOGEN (Nippon Gene Co., Ltd.), was converted into cDNA using a GeneAmp RNA-PCR kit (Thermo Fisher Scientific, Inc.). Reverse transcription was performed at 37˚C for 2 h. qPCR was performed using TB Green Premix Ex Taq II (Takara Bio, Inc.), including TB Green as an intercalator that emits fluorescence when bound to double-stranded DNA. The thermocycling conditions were as follows: 95˚C for 1 min and 50 cycles of 95˚C for 5 sec and 60˚C for 30 sec. Quantification based on the cycle threshold (Ct) values ($2^{-\Delta\Delta Cq}$ method) (10) was performed using an Applied Biosystems 7900 HT Fast Real-time PCR System (Thermo Fisher Scientific, Inc.) as previously described (11). The primers used to amplify the target genes are listed in Table SI. GAPDH was used to normalize the expression levels in quantitative analyses. For the siRNAs listed in Table I, the analyses were conducted once, but in triplicate in case the migration rate was <50%. For a few siRNAs that impaired the viability of the cells, it was not possible to perform the analyses (see below; Table I).

Western blot analysis. Total proteins were extracted from cells using RIPA buffer (FUJIFILM Wako Pure Chemical Corporation) containing protease inhibitor mix Complete™ (Roche Diagnostics). The protein concentrations were determined using a BCA Protein Assay Kit (Pierce; Thermo Fisher Scientific, Inc.). The proteins were boiled at 100˚C, loaded (20 mg per lane), separated by SDS-PAGE (5-20%) and transferred to PVDF membranes. After 1 h of blocking with 3% (w/v) BSA (Merck KGaA) at room temperature, the membranes were incubated overnight with primary antibodies at 4˚C. After being rinsed twice with TBS buffer (pH 8.0) containing 0.1% Tween-20, the membranes were incubated with HRP-labeled secondary antibodies against mouse IgG (100-fold dilution; cat. no. 7076; Cell Signaling Technology, Inc.) at room temperature for 1 h. An enhanced chemiluminescence solution (GE Healthcare) was used for color development. β-actin was used as the internal standard. The experiment was performed in triplicate. Antibodies against protein kinase DNA-activated catalytic subunit (PRKDC)/DNA-dependent protein kinase catalytic subunit (DNA-PK) (1,000-fold dilution; cat. no. 12311; Cell Signaling Technology, Inc.), proteasome subunit β type-4 (PSMB4) (200-fold dilution; cat. no. sc-390878; Santa Cruz Biotechnology, Inc.) and β-actin (200-fold dilution; cat. no. sc-47778; Santa Cruz Biotechnology, Inc.) were used. ImageJ software ver. 1.54 g (National Institutes of Health) was used for densitometry.

Migration assay. The migration assay was performed using the Boyden chamber method using polycarbonate membranes with a pore size of 8 μm (Chemotaxicell; Kurabo Bio-Medical Department; Kurabo Industries, Ltd.) as previously described (11). The membranes were coated with fibronectin (50 μg/ml) on the outer side at room temperature for 1 h and dried for 2 h at room temperature. The cells ($2x10^4$ cells/well) were then seeded into the upper chambers containing 500 μl migrating medium (DMEM containing 0.5% FBS), and the upper chambers were placed into the lower chambers containing 700 μl DMEM with 10% FBS. After incubation at 37˚C for 24 h, the media in the upper chambers were aspirated, and the non-migrated cells on the inner sides of the membranes were removed using a cotton swab. The cells that had migrated to the outer side of the membranes were fixed with 100% ethanol at room temperature for 5 min, stained with 0.1% crystal violet solution at room temperature for 15 min and observed under a light microscope. The number of migrated cells in five fields per chamber was averaged. The migration rate was verified in triplicate for each gene where applicable (Table I).

Selection of genes for the migration assay. The selection of genes was based on our previous expression microarray analysis for CUP (GSE42392) (8), which was compared with microarray datasets for several cancer types obtained from the Gene Expression Omnibus database (https://www.ncbi.nlm.nih.gov/geo/) (12). The datasets used were GSE781 (13), GSE1456 (14), GSE2109 (15), GSE2742 (16), GSE3149 (17), GSE3167 (18), GSE4127 (19), GSE4176 (20), GSE5787 (21), GSE6791 (22) and GSE8218 (23).

Transfection of siRNA. Predesigned siRNAs (MISSION® siRNA) targeting 50 genes and a nonspecific target (MISSION® siRNA Universal Negative Control; Table I) were purchased from MilliporeSigma. Cells were transfected with each siRNA (10 nM) using RNAiMAX (Invitrogen; Thermo Fisher Scientific, Inc.) according to the manufacturer's instructions as previously described (24), incubated at 37˚C for 48 h, and then trypsinized and seeded immediately for the migration assay.

Table I. Effect of siRNA-induced knockdown of genes on cell migration.

		A549 cells			MDA231		
siRNA	siRNA (EHU-)[a]	Viability, %[b]	Fold change of the expression of the gene targeted by the siRNA[c]	Migration rate, %[d]	Viability, %[b]	Fold change of the expression of the gene targeted by the siRNA[c]	Migration rate, %[d]
Control[e]	SIC001	100.0	1.000	100.0	100.0	1.000	100.0
S100A4	125681	>90.0	0.069	>90.0			
HSPA8	115141	>90.0	0.199	>90.0			
TIMP1	156431	>90.0	0.069	>90.0			
LGALS1	034721	>90.0	0.035	>90.0			
SERF2	096201	>90.0	0.559±0.033	44.3±8.1	>90.0	0.652	>90.0
PRKDC	123791	51.0±3.1	0.087±0.020	<1.0	75.2±2.9	0.107±0.018	1.9±1.5
NEDD8	112521	>90.0	0.008	>90.0			
APOC	125971	>90.0	0.314	>90.0			
YWHAZ	076001	>90.0	0.363	>90.0			
SUB1	031131	>90.0	0.037	>90.0			
NOLA3	104671	>90.0	0.044	>90.0			
SNRPD2	146751	50.0±4.6	0.019	67.2±5.4			
ATP5H	128441	>90.0	0.110	>90.0			
TCEB2	150621	>90.0	0.034	71.7±6.9			
OAZ1	034471	>90.0	0.044	>90.0			
NPIPL3	106191	79.3±4.0	0.953	>90.0			
SRGN	143531	>90.0	0.017	>90.0			
S100A6	120391	>90.0	0.019	>90.0			
PFN1	106911	>90.0	0.035	>90.0			
EIF5A	147491	>90.0	0.015	>90.0			
S100A11	147921	46.3±6.4	0.017	55.6±3.9			
NUTF2	159321	64.7±7.1	0.021	50.7±2.5			
STK17A	018811	>90.0	0.167	>90.0			
YWHAH	004271	>90.0	0.096	>90.0			
SELT	117491	>90.0	0.017	>90.0			
CST3	019031	>90.0	0.046	>90.0			
GDI2	109311	>90.0	0.095	>90.0			
VDAC3	108731	>90.0	0.048	>90.0			
TYROBP	033221	>90.0	0.346	>90.0			
VIM	151861	>90.0	0.057	>90.0			
LSM7	057161	>90.0	0.042	>90.0			
GSTP1	009201	>90.0	0.051	>90.0			
NDUFS8	053841	>90.0	0.047	>90.0			
POLR2J	117061	>90.0	0.853	>90.0			
RPS7	110521	25.8±2.1	0.013±0.005	<1.0	<1.0	n.p.	n.p.
RPL11	108131	18.8±3.2	0.002±0.001	<1.0	<1.0	n.p.	n.p.
RPLP2	055751	<1.0	n.p.	n.p.			
RPL18A	147231	<1.0	n.p.	n.p.			
RPL36	056091	<1.0	n.p.	n.p.			
RPS10	110371	<1.0	n.p.	n.p.			
IMP3[f]	085841	58.2±7.4	0.257	>90.0			
CALM3[f]	143521	>90.0	0.023	>90.0			
AP2S1[f]	135191	>90.0	0.009	>90.0			
ARL6IP4[f]	087871	>90.0	0.135	>90.0			

Table I. Continued.

		A549 cells			MDA231		
siRNA	siRNA (EHU-)[a]	Viability, %[b]	Fold change of the expression of the gene targeted by the siRNA[c]	Migration rate, %[d]	Viability, %[b]	Fold change of the expression of the gene targeted by the siRNA[c]	Migration rate, %[d]
ATP6VOB[f]	142591	>90.0	0.038	>90.0			
SH3GLB1[f]	098381	>90.0	0.123±0.011	43.9±6.0	>90.0	0.058	>90.0
CAPNS1[f]	047191	>90.0	0.031±0.009	15.9±2.3	>90.0	0.022	>90.0
PGK1[f]	105941	>90.0	0.232	>90.0			
PSMB4[f]	025191	>90.0	0.051±0.004	21.8±2.5	>90.0	0.033±0.008	17.3±4.3
PDCD6[f]	094521	>90.0	0.030	>90.0			

[a]ID number for MISSION® siRNAs. [b]Ratios of live cells relative to the ratio in the control cells at 72 h after transfection were estimated using an MTT assay conducted in triplicate. [c]Ratios of expression relative to the expression in the control cells were estimated based on reverse transcription-quantitative PCR at 72 h after transfection and verified in triplicate in case the migration rate was <50%. [d]Ratios of migrated cells relative to the control cells were measured based on the migration assay conducted in triplicate. [e]Non-specific target (MISSION® siRNA Universal Negative Control). [f]Genes listed in Table SII. Full descriptions for gene symbols are as listed in Table II in (8) and Table SII. n.p., not performed due to cell viability being <1%; siRNA, small interfering RNA.

Plasmid construction, virus production and stable transfection. shRNAs targeting PRKDC or PSMB4 were constructed using oligonucleotides encoding siRNA directed against the respective genes (5'-CCTGAAGTCTTTACA ACATATCTC-3' and 5'-CCGCAACATCTCTCGCATTAT CTC-3' for PRKDC and PSMB4 shRNA, respectively). The oligonucleotides were cloned into RNAi-Ready pSIREN RetroQZsGreen (Takara Bio, Inc.), which is a self-inactivating retroviral expression vector. This dual expression vector encodes green fluorescent protein (GFP) under the control of the cytomegalovirus promotor and shRNA under the control of the U6 promoter. The viral vectors constructed were designated as pSIREN-shPRKDC, pSIREN-shPSMB4 and a control vector (pSIREN-RetroQZsGreen vector without oligonucleotide inserted). Each of the pSIREN-RetroQZsGreen constructs (45 μg) was co-transfected with a pVSV-G vector (Takara Bio, Inc.) constituting the viral envelope (molar ratio of 3:1 for pSIREN-RetroQZsGreen constructs:pVSV-G vector) into GP2-293 packaging cells ($2x10^7$ cells; Takara Bio, Inc.) using the FuGENE6 transfection reagent (Roche Diagnostics). After 48 h at 37˚C, the culture medium was collected, and the viral particles were concentrated by centrifugation at 15,000 x g for 3 h at 4˚C. The viral pellet was then resuspended in fresh DMEM. The viral vector titer was calculated using a Retrovirus Titer Set (Takara Bio, Inc.) according to the manufacturer's instructions. The minimal MOI was then determined to be 4 for all the constructs by counting the GFP-positive A549 cells infected by serial dilutions of the virus-containing media. At 3 days after the infection with the virus in A549 cells ($1x10^5$ cells), the cells were trypsinized, propagated for 1 week and resuspended in DMEM ($5x10^6$ cells/ml). Subsequently, 1 ml of the resuspended solution was processed for cell sorting using a FACSCalibur Flow Cytometer (BD Biosciences). This device consists of a flow cytometer and a fluorescence activated cell sorter (FACS) in which GFP-positive cells excited by the 488 nm laser line emit green fluorescence at 509 nm, which is optimally detected by the FL-1 detector, and the GFP-positive cells were captured by a catcher tube for sorting (25). The software used for analysis was CellQuest software Ver. 3.3 (BD Biosciences). The subsequent experiment (LN metastasis assay) was performed immediately after the sorted cells reached the number required for inoculation into mice ($1x10^7$ cells for each construct) during the culture for ~1 week.

Animal models and LN metastasis assay. A total of 60 nude mice (BALB/c nu/nu; 5-week-old; female; mean weight, 17.8 g; CLEA Japan, Inc.) were used for the *in vivo* experiments. Experimemts were approved by the Institutional Animal Care Committee of the Kindai University Faculty of Medicine (approval no. KDMS-25-019; Osaka-Sayama, Japan). The mice were housed at the Animal Laboratory, Kindai University Faculty of Medicine (Osaka-Sayama, Japan), and maintained in a specific pathogen-free vivarium at 18-23˚C with 50% humidity under a 12/12 h dark/light cycle. The animals had free access to drinking water and were fed a pelleted basal diet *ad libitum*.

The *in vivo* study consisted of two parts that estimated two effects on the potential of the cells to metastasize from footpad to popliteal LN: Experiment 1, the effect of downregulation of PSMB4 and PRKDC; and experiment 2, the effect of inhibitors of PSMB4 and PRKDC. For each of them, a single experiment was performed and 30 mice were used. For experiment 1, the cells (A549 cells bearing a control vector, pSIREN-shPRKDC, or pSIREN-shPSMB4) were resuspended in Hanks' Balanced Salt Solution (MilliporeSigma) and injected subcutaneously

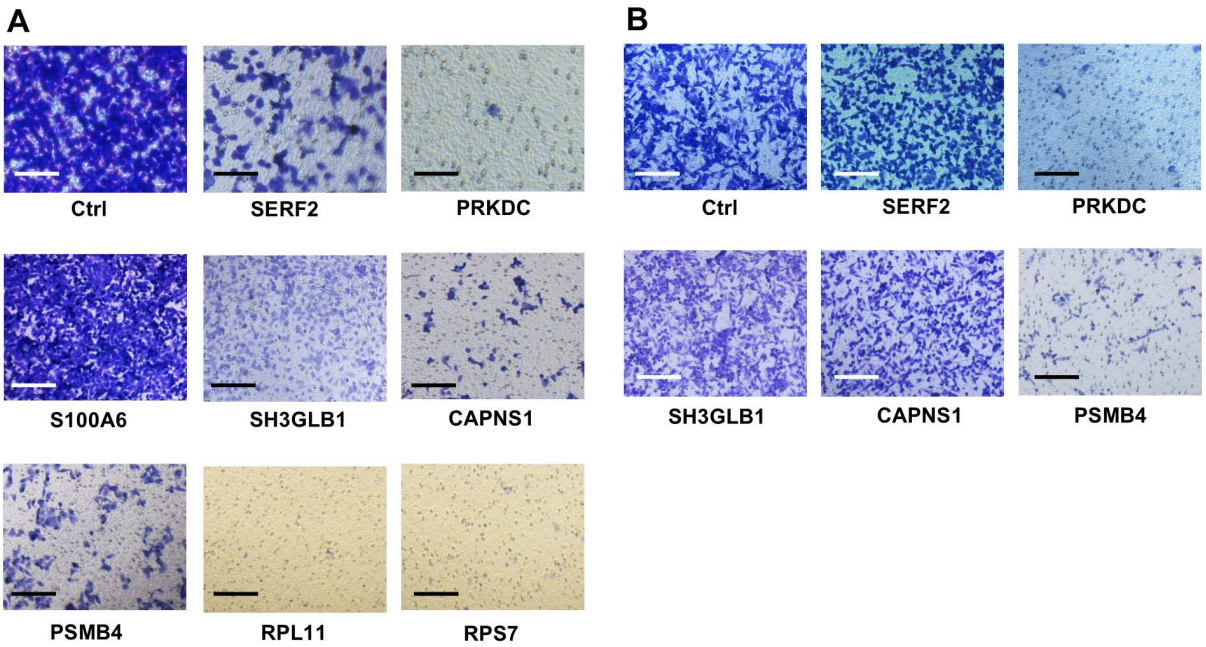

Figure 1. Migration assays were performed using the Boyden chamber method. After transfection of each siRNA into the (A) A549 and (B) MDA231 cells, the cells were incubated for 48 h before the migration assay. The cells that had migrated to the outer side of the membranes within 24 h were fixed and stained. A representative image of a triplicate analysis of each siRNA is shown. Scale bar, 20 μm. siRNA, small interfering RNA; Ctrl, control siRNA; SERF2, small EDRK-rich factor 2; PRKDC, DNA-dependent protein kinase catalytic subunit; S100A6, S100 calcium-binding protein A6; SH3GLB1, SH3-domain GRB2-like endophilin B1; CAPNS1, calpain, small subunit 1; PSMB4, proteasome subunit β type-4; RPL11, ribosomal protein L11; RPS7, ribosomal protein S7.

($1x10^6$ cells) into the hind footpads of mice (10 mice per group) on day 0 in accordance with the method described for a previous study (26). On the final day (day 20), mice were euthanized using CO_2 flowing from a compressed cylinder into a chamber (under ambient conditions) containing the mice so that 100% CO_2 gradually filled the chamber (30%/min) (27). Next, the primary tumors and popliteal LNs were visualized by fluorescence imaging and images were captured using a macro-imaging station consisting of a SBIG cooled CCD camera model ST-7XME (Santa Barbara Imaging) mounted onto a dark box. The integrated density of the fluorescence spots was quantified using ImageJ software ver. 1.54 g (National Institutes of Health). For experiment 2, the DNA-PK inhibitor NU7441 (10 mg/kg; FUJIFILM Wako Pure Chemical Corporation) (28) and the proteasome inhibitor bortezomib (1 mg/kg; Takeda Pharmaceutical Company, Ltd.) (29), and vehicle (DMSO) were administered intravenously alone (9-10 mice/group) 1 week after inoculation of A549 cells bearing a control vector, and this administration was repeated twice a week for 3 weeks (2nd to 4th weeks). The LNs were resected (on day 35), and their maximum diameters were measured. Fluorescence images were also captured for the primary tumors and popliteal LNs. The animal details and protocol were otherwise as aforementioned.

Statistical analysis. Data are presented as the mean ± SD, unless otherwise noted. An unpaired t-test was used for comparisons between two groups. Comparisons among multiple groups were conducted using one-way ANOVA, followed by the Student-Newman-Keuls test. These analyses were performed as a single experiment. Statistical analyses were performed using SigmaPlot v13.0 (Grafiti LLC). $P<0.05$ was considered to indicate a statistically significant difference.

Results

Selection of candidate genes in CUP. In our previous microarray study, 44 genes that were upregulated in CUPs compared with non-CUPs as a whole were identified (8). Of the 44 genes, 40 were selected as candidates for the next screening using the migration assay (Table I). Three pseudogene-like genes (LOC392501, LOC442171 and LOC646417) with unknown functions and one gene without an available siRNA (LAPTM5) were excluded. As additional candidates for the screening, 10 genes that were screened out by the comparison of gene expression profiles between CUP and individual cancer types of known primary site were selected (8). These 10 genes were most highly expressed in CUP of all cancer types examined, and each of the genes showed ≥1.5-fold enriched expression in CUP compared with the second most enriched cancer type for each gene (Table SII). A total of 50 genes were selected (Table I) for the migration assay.

Screening for genes associated with the metastatic potential in CUP. For all 50 aforementioned genes, specific siRNAs were obtained from the same commercial source (MISSION® siRNA; Table I). For screening, A549 cells were transfected with siRNAs, and genes were evaluated for suppressed migration after siRNA knockdown. Images for cell migration assays are shown in Figs. 1 and S1. The migration assay showed that A549 cells transfected with some siRNAs exhibited poor migration, meaning the number of A549 cells migrating to the outer side of the porous membrane in the Boyden chamber was decreased compared with that of the cells transfected with control siRNA (Fig. 1A). For each of the 50 siRNAs transfected into A549 cells, the present study aimed to determine the cell viability, the fold-change in the expression of the targeted

gene and the cell migration rate (Table I). The results revealed that transfection with siRNAs targeting SERF2, PRKDC, SH3GLB1, CAPNS1, PSMB4, RPS7 and RPL11 reduced the migration of A549 cells by >50% (Fig. 1A; Table I).

Our previous study identified six genes encoding ribosomal proteins (RPLP2, RPL18A, RPL36, RPS10, RPS7 and RPL11) as CUP-associated (-upregulated) genes (8). siRNAs against four of these ribosomal protein genes (RPLP2, RPL18A, RPL36 and RPS10) almost completely impaired the viability of A549 cells, and it was not possible to perform the expression assay and migration assay using siRNAs of these genes (Table I). The other two siRNAs (targeting RPS7 and RPL11) abolished the viability of MDA231 cells (Table I), indicating that reduced expression of any single ribosomal protein molecule could be critical for cell survival.

The present study subsequently focused on the siRNAs against the five genes (SERF2, PRKDC, SH3GLB1, CAPNS1 and PSMB4) based on their ability to reduce migration to less than half of that of the control without affecting the cell viability (>50% of the control; Table I). The present study further analyzed their influence on the migration of another cell line (MDA231). Only siRNAs specific for PRKDC and PSMB4 markedly reduced the migration of the cells (Fig. 1B; Table I). These siRNAs did not affect the viability of MDA231 cells, resulting in a cell viability rate of 75.2% for PRKDC-specific siRNA and >90% for PSMB4-specific siRNA. Furthermore, a marked reduction in the expression of the respective genes was observed. The siRNAs targeting PRKDC and PSMB4 reduced the expression levels of the corresponding genes (0.107- and 0.033-fold changes, respectively), which was similar to the trends observed for A549 cells (Table I). Western blotting confirmed that the expression of PRKDC and PSMB4 was reduced by the siRNA-induced mRNA knockdown (Fig. 2).

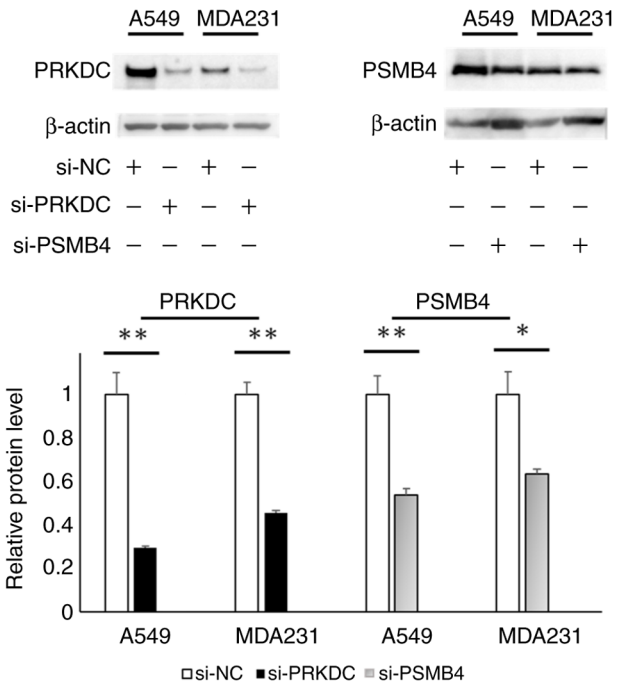

Figure 2. Western blotting showing the reduction in protein expression following siRNA-induced knockdown of PRKDC and PSMB4. (Top) Protein expression was reduced after transfection of the cells with siRNA for PRKDC (left) and PSMB4 (right) in both the A549 and MDA231 cells. β-actin was used as the loading control, whereas si-NC was used as the negative control. (Bottom) Relative reductions in PRKDC or PSMB4 protein expression were determined using western blot analysis conducted in triplicate. Data are presented as the mean and standard deviation. *P<0.05; **P<0.01. siRNA/si, small interfering RNA; si-NC, siRNA universal negative control; PRKDC, DNA-dependent protein kinase catalytic subunit; PSMB4, proteasome subunit β type-4.

Effect of downregulation of the candidate genes on LN metastasis. To determine whether downregulation of the two genes, PRKDC and PSMB4, might affect the potential of the cells to metastasize to the LNs *in vivo*, cell lines that stably expressed both GFP and shRNA targeting the respective genes were engineered. A control cell line transfected with a control vector that expressed GFP alone was also established. The stable cell lines for these constructs were isolated by FACS using GFP as a reporter (Fig. S2A-C) and they showed stable shRNA-based knockdown of PRKDC and PSMB4 during the passage culture for ≥3 months. Western blotting confirmed that the PRKDC and PSMB4 proteins expressed in A549 cells were reduced for the respective constructs compared with the control vector (Fig. S3A). The growth rate remained unaltered in the A549 cells transfected with shRNA targeting PSMB4 (>90% of the rate in the control cells), but the cells transfected with shRNA targeting PRKDC exhibited an ~25% reduction in the growth rate relative to that in the control cells at 72 h (Fig. S3B). To evaluate the metastasis-promoting potential of these two genes, cells ($1x10^6$) containing the respective shRNA constructs were subcutaneously injected into the footpads of BALB/c nude mice. On day 20, the fluorescence intensities of GFP expressed in the footpad and popliteal LNs were measured (Fig. 3A). The fluorescence intensities were lower after injection of cells expressing PRKDC-shRNA than after injection of cells transfected with a control vector (~14.8%), whereas fluorescence intensities following injection of the cells expressing PSMB4-shRNA were comparable to those following injection of cells containing the control vector (Fig. 3B and C). A proportionate reduction in fluorescence intensities was also observed in the popliteal LNs in both the PRKDC-shRNA and PSMB4-shRNA groups, with popliteal LN/footpad fluorescence intensity ratios of 39.4 and 45.5%, respectively, compared with the control group (Fig. 3C). It was attempted to perform a similar assay using MDA231-shRNA constructs; however, this cell line failed to become engrafted into the footpads of the mice (data not shown).

The present study subsequently examined whether known inhibitors of PRKDC (DNA-PK) or PSMB4 (proteasome) could alter the migration of cells. The inhibitors were injected intravenously into the tails of mice that had been inoculated with A549 cells harboring a control vector expressing GFP. NU7441, a DNA-PK inhibitor, did not significantly change the fluorescence intensity in either the footpads or popliteal LNs (Fig. 4A and B). By contrast, bortezomib, a proteasome inhibitor, markedly retarded the migration of the cells to the popliteal LNs, although the cell growth rate in the footpads was comparable to that in the control animals, resulting in a lower popliteal/footpad fluorescence intensity ratio compared with that in the control

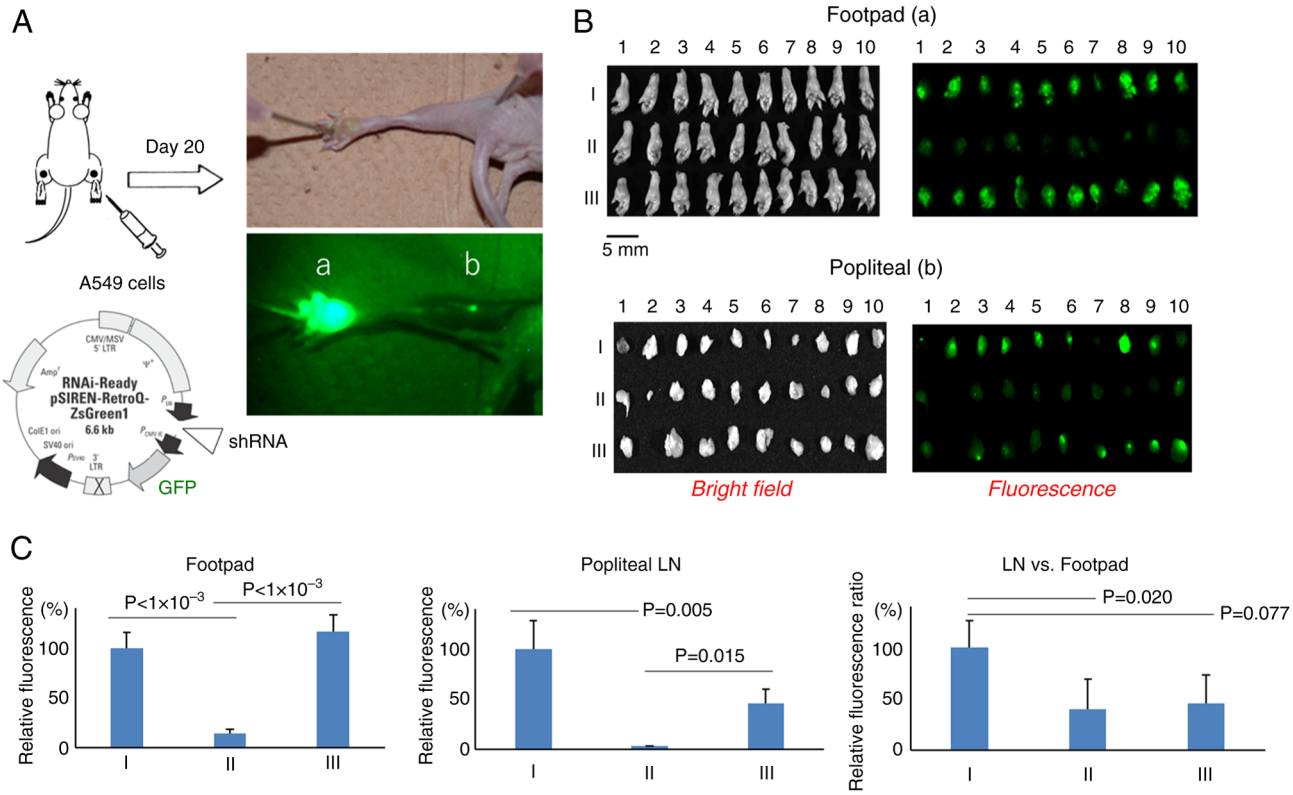

Figure 3. Quantification of cells migrating from the footpad to the popliteal LNs. (A) On day 20 after inoculation of the cells into the footpad, the mice were sacrificed and fixed, and the fluorescence in the (a) footpad and (b) LNs was visualized and quantified. (B) Bright-field images (left) and fluorescence images (right) of the resected footpad (top) and LNs (bottom) are shown for: I, A549 cells harboring a control vector; II, A549 cells expressing PRKDC shRNA; and III, A549 cells expressing PSMB4 shRNA. Scale bar, 5 mm. (C) Relative fluorescence levels of control vector (I), PRKDC shRNA (II) and PSMB4 shRNA (III) in the footpad (left) and LN (middle), and the LN/footpad fluorescence ratio (right). Data are presented as the mean ± standard error of the mean. LN, lymph node; PRKDC, DNA-dependent protein kinase catalytic subunit; PSMB4, proteasome subunit β type-4; shRNA, short hairpin RNA; GFP, green fluorescent protein.

group (P=0.093) and in the animals injected with NU7441 (P=0.017) (Fig. 4B).

A marked difference in the size of the metastatic LNs was observed between the groups that were and were not treated with bortezomib (Fig. 4C). Compared with the control group (vehicle), the bortezomib-treated group showed significantly smaller (undeveloped) tumors at the metastatic sites (LNs; $P<10^{-4}$). The mean LN maximum diameters in the group treated with vehicle and in the group treated with NU7447 (DNA-PK inhibitor) were 6.3- and 4.5-fold greater than the diameter of intact LNs, whereas they were only 1.4-fold greater in the group treated with bortezomib.

Discussion

Our previous study analyzed tumor mRNA samples from 60 patients with CUP using microarray analysis and constructed a normalized gene expression profile specific to CUPs, which identified a number of genes that were upregulated in the CUP (8).

In the present study, to further narrow down the genes closely related to the development of CUP among these candidate genes, cell-based siRNA screening was performed *in vitro*. A549 and MDA231 cells were selected for the screening because they are among the most widely used cell lines as models for research on the metastasis of lung cancer and breast cancer, respectively (30,31). Furthermore, our previous study demonstrated that the gene expression profile of CUP closely resembled that of lung adenocarcinoma (8).

Individual knockdown of several candidate genes in A549 or MDA231 cells using specific siRNAs resulted in restricted migration of the cells. siRNAs against PRKDC and PSMB4 restricted the migration in both cell lines, suggesting that these genes might be involved in the metastatic ability of CUP. Furthermore, shRNAs for PRKDC and PSMB4 also suppressed the migration of A549 cells *in vivo*, with significance observed for shRNA for PRKDC, whereas knockdown of PRKDC tended to slow the growth of the cells as well. The PRKDC gene encodes DNA-PKcs, a large subunit (~469 KDa) of DNA-PK, which is an abundantly expressed kinase in higher eukaryotes (32). As a DNA damage repair protein, it drives several pathways that promote metastasis and tumor growth (33,34). In melanoma cells, DNA-PKcs may control the secretion of numerous proteins involved in metastasis, such as matrix metalloproteinases, thereby regulating the tumor microenvironment (35). A similar regulation in favor of metastasis could occur in CUPs exhibiting upregulation of DNA-PKcs (8).

PSMB4 encodes the β7 subunit of proteasome 20S. The 20S proteasome is the catalytic core of the proteasome complex with a concentric circular structure, including two α rings and two β rings, each ring consisting of 7 subunits, α1-7

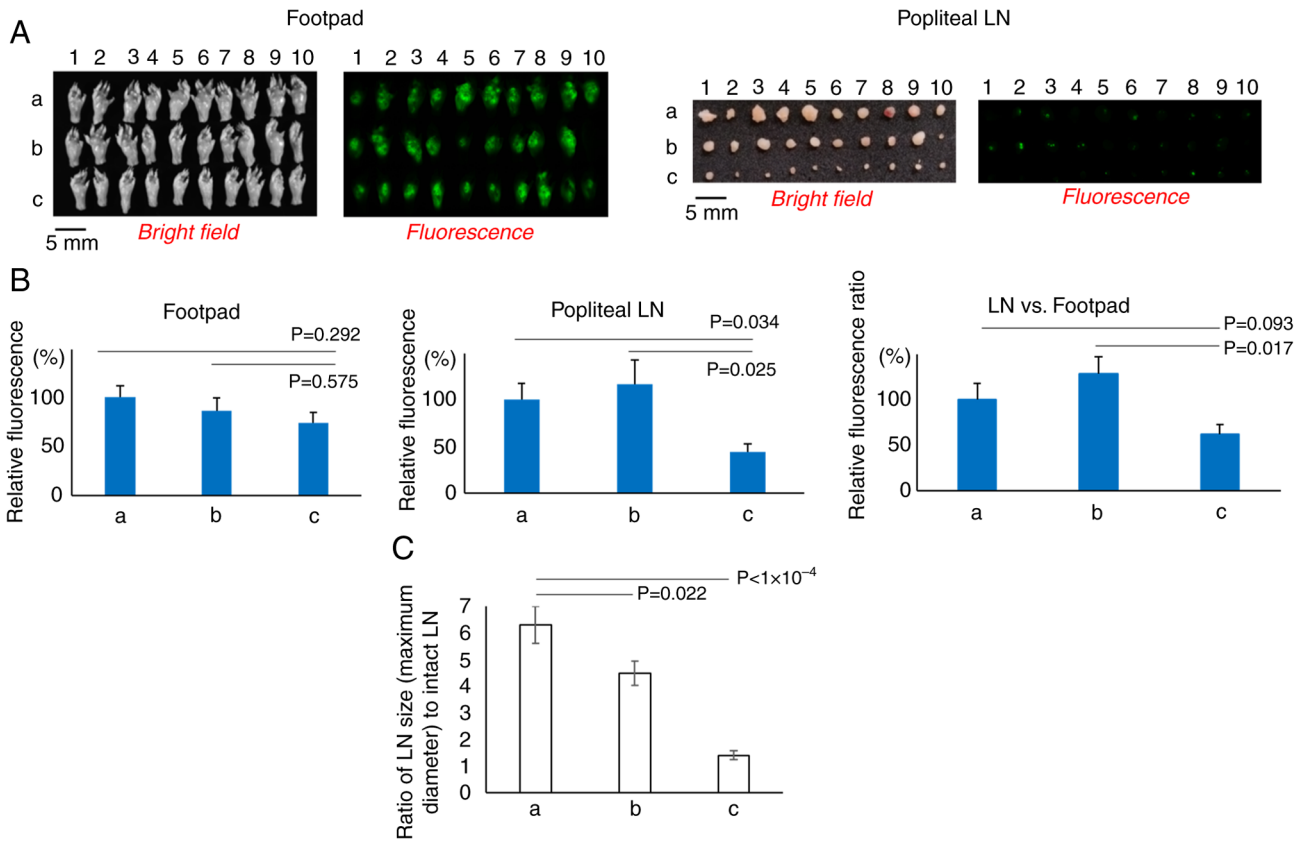

Figure 4. Effect of inhibitors on the migration of the A549 cells. (A) Mice inoculated with A549 cells harboring a vector expressing green fluorescent protein were treated with (a) vehicle, (b) Nu7447 (protein kinase, DNA-activated, catalytic polypeptide inhibitor) or (c) bortezomib (a proteasome inhibitor) twice a week from week 2 to week 4. On day 35 after inoculation, mice were sacrificed and fixed, and fluorescence intensities in the footpads and popliteal LNs were visualized. The bright field and fluorescence images are shown. One mouse (b-10) was excluded from the quantification due to absence of a tumor (likely due to technical error) whose footpad and LN are each shown as an intact sample. Scale bar, 5 mm. (B) Fluorescence intensities relative to the control in the footpad (left) and LNs (middle), and the LN/footpad fluorescence intensity ratio (right) in the animals treated with vehicle (a), Nu7447 (b) and bortezomib (c). (C) Relative size of metastatic tumors in the LN. The ratio of LN sizes (maximum diameter) to intact LN [b-10 in (A)] was calculated for mice treated with (a-c) as in (B). Data are presented as the mean ± standard error of the mean. LN, lymph node.

and β1-7, respectively (36). Proteasomes affect tumor development by regulating tumor signaling pathways, including NF-κB signaling. They recognize and degrade ubiquitinated IκB, an inhibitor of NF-κB, thereby activating NF-κB signaling (37). Proteasomes are also required to maintain homeostasis in proliferating tumor cells by eliminating the accumulation of misfolded proteins (38). In multiple myeloma (MM), plasma cells secrete several immunoglobulins, which are macromolecules that are synthesized and folded in the endoplasmic reticulum (ER) (36). Therefore, proteasome inhibitors that are widely used in the treatment of MM can block the degradation of IκB and trigger the accumulation of misfolded proteins, inhibiting NF-κB activity and inducing ER stress, respectively, ultimately leading to cell death of the MM cells (39,40). Furthermore, DNA-PKcs is an additional target that is cleaved and inactivated by proteasome inhibitors in MM cells (40,41).

In the present study, bortezomib, the first proteasome inhibitor developed as a chemotherapy drug (29), markedly restricted the metastatic ability of A549 cells *in vivo*. The target of this drug has been identified as the β5 subunit of proteasome 20S (39). Subunits other than the β7 subunit (encoded by *PSMB4*) include the β5 subunit, which was also upregulated in both CUPs (GSE42392) (8) and A549 cells compared with small airway epithelial cells (GSE4824) (42) (Table SIII). The trend was also noted in other tumors located in the liver or head and neck regions (Table SIII), with each of these tumors identified as a potential treatment target for bortezomib (36,37).

The development of immune checkpoint inhibitors (ICIs) has markedly changed the treatment paradigms for numerous cancer types. Among patients with CUP, 28% exhibit one or more predictive biomarkers for ICIs. For example, programmed death-ligand 1 is expressed on ≥5% tumor cells in 22.5% or on lymphocytes in 58.7% of such patients. Microsatellite instability-high is observed in 1.8% and tumor mutational burden (TMB) ≥17 mutations per megabase of the tumor genome is present in 11.8% of these patients (43).

Although these biomarkers have not yet been validated in patients with CUP, those with CUP with TMB >10 mutations per megabase generally experience improved outcomes when treated with ICIs (43), and our previous study recently demonstrated the clinical benefits of nivolumab in patients with CUP (44). The present study demonstrated a putative role for the proteasome in the progression of CUP that could be prevented by proteasome-targeted therapy. Proteasome inhibitors combined with ICIs may be an additional therapeutic option for CUP, for which there are limited treatment options.

Acknowledgements

The authors would like to thank Mrs. Tomoko Kitayama (Department of Genome Biology, Kindai University Faculty of Medicine, Osaka-Sayama, Japan) and Mr. Kentaro Egawa (Center for Animal Experiment, Kindai University Faculty of Medicine, Osaka-Sayama, Japan) for help with the animal experiments.

Funding

The present study was supported by the Grant-in-Aid for Scientific Research (C) (grant no. 17K07204) of Ministry of Education, Culture, Sports, Science and Technology of Japan, and by the Japan Agency for Medical Research and Development (grant no. 201438137A).

Availability of data and materials

The data generated in the present study may be requested from the corresponding author.

Authors' contributions

YF designed the study and drafted the manuscript. YF and MADV performed the experiments and collected data. YF, MADV, HH, KNa and KNi analyzed and interpreted the data, and revised the manuscript. YF and MADV confirmed the authenticity of all the raw data. All authors have read and approved the final version of the manuscript.

Ethics approval and consent to participate

The present study was approved by the Institutional Animal Care Committee of the Kindai University Faculty of Medicine (approval no. KDMS-25-019; Osaka-Sayama, Japan) and carried out in compliance with the standards for the use of laboratory animals.

Patient consent for publication

Not applicable.

Competing interests

The authors declare that they have no competing interests.

References

1. Pavlidis N and Pentheroudakis G: Cancer of unknown primary site. Lancet 379: 1428-1435, 2012.
2. Rassy E, Parent P, Lefort F, Boussios S, Baciarello G and Pavlidis N: New rising entities in cancer of unknown primary: Is there a real therapeutic benefit? Crit Rev Oncol Hematol 147: 102882, 2020.
3. Greco FA and Pavlidis N: Treatment for patients with unknown primary carcinoma and unfavorable prognostic factors. Semin Oncol 36: 65-74, 2009.
4. Pavlidis N, Khaled H and Gaafar R: A mini review on cancer of unknown primary site: A clinical puzzle for the oncologists. J Adv Res 6: 375-382, 2015.
5. Fizazi K, Greco FA, Pavlidis N, Daugaard G, Oien K and Pentheroudakis G; ESMO Guidelines Committee: Cancers of unknown primary site: ESMO clinical practice guidelines for diagnosis, treatment and follow-up. Ann Oncol 26 (Suppl 5): v133-v138, 2015.
6. Hayashi H, Kurata T, Takiguchi Y, Arai M, Takeda K, Akiyoshi K, Matsumoto K, Onoe T, Mukai H, Matsubara N, *et al*: Randomized phase II trial comparing site-specific treatment based on gene expression profiling with carboplatin and paclitaxel for patients with cancer of unknown primary site. J Clin Oncol 37: 570-579, 2019.
7. Rassy E, Labaki C, Chebel R, Boussios S, Smith-Gagen J, Greco FA and Pavlidis N: Systematic review of the CUP trials characteristics and perspectives for next-generation studies. Cancer Treat Rev 107: 102407, 2022.
8. Kurahashi I, Fujita Y, Arao T, Kurata T, Koh Y, Sakai K, Matsumoto K, Tanioka M, Takeda K, Takiguchi Y, *et al*: A microarray-based gene expression analysis to identify diagnostic biomarkers for unknown primary cancer. PLoS One 8: e63249, 2013.
9. Arao T, Fukumoto H, Takeda M, Tamura T, Saijo N and Nishio K: Small in-frame deletion in the epidermal growth factor receptor as a target for ZD6474. Cancer Res 64: 9101-9104, 2004.
10. Livak KJ and Schmittgen TD: Analysis of relative gene expression data using real-time quantitative PCR and the 2(-Delta Delta C(T)) method. Methods 25: 402-408, 2001.
11. Tanaka K, Arao T, Maegawa M, Matsumoto K, Kaneda H, Kudo K, Fujita Y, Yokote H, Yanagihara K, Yamada Y, *et al*: SRPX2 is overexpressed in gastric cancer and promotes cellular migration and adhesion. Int J Cancer 124: 1072-1080, 2009.
12. Clough E and Barrett T: The gene expression omnibus database. Methods Mol Biol 1418: 93-110, 2016.
13. Lenburg ME, Liou LS, Gerry NP, Frampton GM, Cohen HT and Christman MF: Previously unidentified changes in renal cell carcinoma gene expression identified by parametric analysis of microarray data. BMC Cancer 3: 31, 2003.
14. Pawitan Y, Bjöhle J, Amler L, Borg AL, Egyhazi S, Hall P, Han X, Holmberg L, Huang F, Klaar S, *et al*: Gene expression profiling spares early breast cancer patients from adjuvant therapy: Derived and validated in two population-based cohorts. Breast Cancer Res 7: R953-R964, 2005.
15. International Genetics Consortium: Expression project for oncology (expO). Gene Expression Omnibus, GSE2109, 2005. Available from: http://www.intgen.org/.
16. Luesch H, Chanda SK, Raya RM, DeJesus PD, Orth AP, Walker JR, Belmonte JCI and Schultz PG: A functional genomics approach to the mode of action of apratoxin A. Nat Chem Biol 2: 158-167, 2006.
17. Bild AH, Yao G, Chang JT, Wang Q, Potti A, Chasse D, Joshi NR, Harpole D, Lancaster JM, Berchuck A, *et al*: Oncogenic pathway signatures in human cancers as a guide to targeted therapies. Nature 439: 353-357, 2006.
18. Dyrskjøt L, Kruhøffer M, Thykjaer T, Marcussen N, Jensen JL, Møller K and Ørntoft TF: Gene expression in the urinary bladder: A common carcinoma in situ gene expression signature exists disregarding histopathological classification. Cancer Res 64: 4040-4048, 2004.
19. Gemma A, Li C, Sugiyama Y, Matsuda K, Seike Y, Kosaihira S, Minegishi Y, Noro R, Nara M, Seike M, *et al*: Anticancer drug clustering in lung cancer based on gene expression profiles and sensitivity database. BMC Cancer 6: 174, 2006.
20. Rinaldi A, Kwee I, Taborelli M, Largo C, Uccella S, Martin V, Poretti G, Gaidano G, Calabrese G, Martinelli G, *et al*: Genomic and expression profiling identifies the B-cell associated tyrosine kinase Syk as a possible therapeutic target in mantle cell lymphoma. Br J Haematol 132: 303-316, 2006.
21. Bachtiary B, Boutros PC, Pintilie M, Shi W, Bastianutto C, Li JH, Schwock J, Zhang W, Penn LZ, Jurisica I, *et al*: Gene expression profiling in cervical cancer: An exploration of intratumor heterogeneity. Clin Cancer Res 12: 5632-5640, 2006.
22. Pyeon D, Newton MA, Lambert PF, den Boon JA, Sengupta S, Marsit CJ, Woodworth CD, Connor JP, Haugen TH, Smith EM, *et al*: Fundamental differences in cell cycle deregulation in human papillomavirus-positive and human papillomavirus-negative head/neck and cervical cancers. Cancer Res 67: 4605-4619, 2007.
23. Wang Y, Xia XQ, Jia Z, Sawyers A, Yao H, Wang-Rodriquez J, Mercola D and McClelland M: In silico estimates of tissue components in surgical samples based on expression profiling data. Cancer Res 70: 6448-6455, 2010.
24. Kaneda H, Arao T, Tanaka K, Tamura D, Aomatsu K, Kudo K, Sakai K, De Velasco MA, Matsumoto K, Fujita Y, *et al*: FOXQ1 is overexpressed in colorectal cancer and enhances tumorigenicity and tumor growth. Cancer Res 70: 2053-2063, 2010.
25. Picot J, Guerin CL, Le Van Kim C and Boulanger CM: Flow cytometry: Retrospective, fundamentals and recent instrumentation. Cytotechnology 64: 109-130, 2012.

26. Chen Z, Zhuo W, Wang Y, Ao X and An J: Down-regulation of layilin, a novel hyaluronan receptor, via RNA interference, inhibits invasion and lymphatic metastasis of human lung A549 cells. Biotechnol Appl Biochem 50: 89-96, 2008.
27. Kura Y, De Velasco MA, Sakai K, Uemura H, Fujita K and Nishio K: Exploring the relationship between ulcerative colitis, colorectal cancer, and prostate cancer. Hum Cell 37: 1706-1718, 2024.
28. Zhao Y, Thomas HD, Batey A, Cowell IG, Richardson CJ, Griffin RJ, Calvert AH, Newell DR, Smith GCM and Curtin NJ: Preclinical evaluation of a potent novel DNA-dependent protein kinase inhibitor NU7441. Cancer Res 66: 5354-5362, 2006.
29. Chen D, Frezza M, Schmitt S, Kanwar J and Dou QP: Bortezomib as the first proteasome inhibitor anticancer drug: Current status and future perspectives. Curr Cancer Drug Targets 11: 239-253, 2011.
30. Lengrand J, Pastushenko I, Vanuytven S, Song Y, Venet D, Sarate RM, Bellina M, Moers V, Boinet A, Sifrim A, *et al*: Pharmacological targeting netrin-1 inhibits EMT in cancer. Nature 620: 402-408, 2023.
31. Liu K, Newbury PA, Glicksberg BS, Zeng WZD, Paithankar S, Andrechek ER and Chen B: Evaluating cell lines as models for metastatic breast cancer through integrative analysis of genomic data. Nat Commun 10: 2138, 2019.
32. Dylgjeri E and Knudsen KE: DNA-PKcs: A targetable protumorigenic protein kinase. Cancer Res 82: 523-533, 2022.
33. Xiang Z, Hou G, Zheng S, Lu M, Li T, Lin Q, Liu H, Wang X, Guan T, Wei Y, *et al*: ER-associated degradation ligase HRD1 links ER stress to DNA damage repair by modulating the activity of DNA-PKcs. Proc Natl Acad Sci USA 121: e2403038121, 2024.
34. Caron P, Pankotai T, Wiegant WW, Tollenaere MAX, Furst A, Bonhomme C, Helfricht A, de Groot A, Pastink A, Vertegaal ACO, *et al*: WWP2 ubiquitylates RNA polymerase II for DNA-PK-dependent transcription arrest and repair at DNA breaks. Genes Dev 33:684-704, 2019.
35. Kotula E, Berthault N, Agrario C, Lienafa MC, Simon A, Dingli F, Loew D, Sibut V, Saule S and Dutreix M: DNA-PKcs plays role in cancer metastasis through regulation of secreted proteins involved in migration and invasion. Cell Cycle 14: 1961-1972, 2015.
36. Zhou X, Xu R, Wu Y, Zhou L and Xiang T: The role of proteasomes in tumorigenesis. Genes Dis 11: 101070, 2023.
37. Narayanan S, Cai CY, Assaraf YG, Guo HQ, Cui Q, Wei L, Huang JJ, Ashby CR Jr and Chen ZS: Targeting the ubiquitin-proteasome pathway to overcome anti-cancer drug resistance. Drug Resist Updat 48: 100663, 2020.
38. Chhabra S: Novel proteasome inhibitors and histone deacetylase inhibitors: Progress in myeloma therapeutics. Pharmaceuticals (Basel) 10: 40, 2017.
39. Gandolfi S, Laubach JP, Hideshima T, Chauhan D, Anderson KC and Richardson PG: The proteasome and proteasome inhibitors in multiple myeloma. Cancer Metastasis Rev 36: 561-584, 2017.
40. Hideshima T and Anderson KC: Biologic impact of proteasome inhibition in multiple myeloma cells-from the aspects of preclinical studies. Semin Hematol 49: 223-227, 2012.
41. Wu YH, Hong CW, Wang YC, Huang WJ, Yeh YL, Wang BJ, Wang YJ and Chiu HW: A novel histone deacetylase inhibitor TMU-35435 enhances etoposide cytotoxicity through the proteasomal degradation of DNA-PKcs in triple-negative breast cancer. Cancer Lett 400: 79-88, 2017.
42. Byers LA, Diao L, Wang J, Saintigny P, Girard L, Peyton M, Shen L, Fan Y, Giri U, Tumula PK, *et al*: An epithelial-mesenchymal transition gene signature predicts resistance to EGFR and PI3K inhibitors and identifies Axl as a therapeutic target for overcoming EGFR inhibitor resistance. Clin Cancer Res 19: 279-290, 2013.
43. Rassy E, Boussios S and Pavlidis N: Genomic correlates of response and resistance to immune checkpoint inhibitors in carcinomas of unknown primary. Eur J Clin Invest 51: e13583, 2021.
44. Tanizaki J, Yonemori K, Akiyoshi K, Minami H, Ueda H, Takiguchi Y, Miura Y, Segawa Y, Takahashi S, Iwamoto Y, *et al*: Open-label phase II study of the efficacy of nivolumab for cancer of unknown primary. Ann Oncol 33: 216-226, 2022.